JREE: Vol. 2, No.2, (Spring 2015) 47-58

Journal of Renewable Energy and Environment

Research Article

Journal Homepage: www.jree.ir

Multi-objective Optimization of PV-SOFC-GT-Electrolyser Hybrid System

S. Sadeghi[a]*, M. Ameri[b]

[a]Department of Mechanical Engineering, Graduate University of Advanced Technology, Kerman, Iran
[b]Department of Mechanical Engineering, Shahid Bahonar University, Kerman, Iran

PAPER INFO

Paper history:
Received 09 May 2015
Accepted in revised form 21 September 2015

Keywords:
PV
SOFC-GT
electrolyser
multi-objective
hybrid system

ABSTRACT

This study shows the design of a new hybrid power generation system, photovoltaic panel (PV)–coupled solid oxide fuel cell (SOFC) and gas turbine (GT)–electrolyser. Three objectives (cost, pollutant emissions, and reliability), which are usually in conflict, are considered simultaneously. The design of a hybrid system, considering the three mentioned objectives, poses a very complex problem of optimization. A multi-objective optimization method (PESA) is considered to obtain the best combinations for the hybrid system. In this work, the effect of panel's angle change and SOFC-GT fuel type are considered too. In order to study the effect of fuel price, this study is done about two fuel prices: Iran fuel price and international fuel price.

1. INTRODUCTION

Nowadays, satisfying the energy demand is a sensitive global topic. In parallel, it is also necessary to limit fossil fuels consumption for both sustainability and energy self-sufficiency issues. Therefore, in the global warming context, the development of intermittent renewable energy like photovoltaic (PV) could partly respond to the long term prospects of an increasing energy demand. The conversion of solar is clean, silent and reliable, with reduced maintenance costs, and with small ecological impact. Moreover, sunlight is for free, practically inexhaustible and involves no polluting residues or greenhouse gases emission. Along with these advantages, the electric power production systems using as primary sources exclusively the solar, pose technical problems due to day–night–summer–winter alternation. Such systems would be especially adapted when coupled with a storage system and an auxiliary system that would both increase the productivity of power plants and reduce the areas dedicated to energy production. Such systems, dedicated to decentralized production of electric power based on combined sources of energy, are called hybrid systems. Baniasad Askari and Ameri [1] studied a simple optimization method for calculating the optimum configurations of photovoltaic–battery (PV–bat) hybrid system with high reliability and minimum cost. The proposed method was applied to design a PV–bat system to supply a typical load requirement in a remote region in Kerman, Iran.

Nafeh [2] sized a PV/Diesel generator hybrid energy system to meet the load for about 100% availability. The operation of the diesel generator and the number of the PV modules and batteries were optimized for a given load characteristic and a given diesel generator that would achieve a minimum initial cost and a desired depth of discharge for battery storage. Dufo and Bernal [3] optimized a PV-Diesel system by HOGA program (Hybrid Optimization by Genetic Algorithms) and compared it with a stand-alone PV-only system. Results show the economical advantages of the PV-hybrid system. Morega and Tudorache [4] designed an optimal integrated hybrid system for autonomous electric power production, based on the concurrent operation of a wind turbine and a Photovoltaic (PV) system, backuped by a diesel generator. The optimization of the proposed hybrid system is based on the logistic type numerical models implemented in the HOMER software package.

Rehman and Al-Hadhrami [5] studied a PV-diesel hybrid power system with battery backup for a village being fed by diesel generated electricity to replace part of the diesel by solar. Four generators of different rated powers, diesel prices of 0.2-1.2US$/lit, different sizes of batteries and converters were used to find an optimal power system for the village. Khatib et al [6] performed an optimization to build an integrated hybrid PV/diesel generator system for zero load rejection for Malaysia.

*Corresponding Author's Email: s.sadeghi@kgut.ac.ir(S.Sadeghi)

The optimization presented in their work aims to calculate the optimum capacities of a PV array and diesel generator, which investigates the minimum system cost. Yamegueu et al [7] studied the results of an experimental study of a PV/diesel hybrid system without storage. Their experimental results showed that the sizing of a PV/diesel hybrid system by taking into account the solar radiation and the load/demand profile of a typical area may lead the diesel generator to operate near its optimal point. Also, for a reliability of a PV/diesel hybrid system, the rated power of the diesel generator should be equal to the peak load. Baniasad and Ameri [8] used PV-diesel-battery power systems to meet typical load requirements in a remote region in Kerman, Iran. They used a simple optimization method to determine systems with high reliability and low cost.

The combination of solar panels with fuel cells and electrolyser is often studied, but usually Proton exchange membrane (PEM) fuel cells are used. Nbil et al [9] presented a hybrid energy system combining variable speed wind turbine, solar photovoltaic, electrolyser, and PEM fuel cell generation systems to supply continuous power to residential power applications as stand-alone loads. Silva et al [10] presented an economical assessment and optimization of a hybrid distributed generation system, comprised of a PV system, PEM fuel cell, and batteries as a potential source of energy for isolated communities in the Amazon region. Eroglu et al [11] proposed a photovoltaic/wind/electrolyser/PEM fuel cell hybrid power system for stand-alone applications demonstrated by a mobile house. They showed that different renewable sources can be used simultaneously to power off-grid applications. Lee et al [12] described the Power managements of a UAV's hybrid electric propulsion systems. They considered three electric propulsion systems with different power sources, i.e. solar cells, fuel cells, and batteries. Each power source was modelled in Matlab/Simulink and integrated into the power system. Fuel cells and batteries simulation processes were verified via a comparison between the simulation results and available flight test results of UAVs. Sadeghi and Ameri [13] compared the combination of different auxiliary systems with solar panels and batteries in terms of economical efficiency, ecological compatibility, and reliability. Auxiliary systems include diesel generator, gas generator, solid oxide fuel cell, and micro gas turbine. They also considered the effect of fuel price, technology development in SOFC cost, changes in the power of auxiliary power system and also change in the maximum number of panels. Because of high temperature products, SOFCs are suitable to combine with gas turbine or micro gas turbine. Cheddie [14] indirectly coupled the SOFC system to the GT in order to minimize the disruption to the GT operation. Santin et al [15] considered a study of SOFC–GT hybrids for operation with liquid fuels. Two liquid fuels were investigated, methanol and kerosene, in four layouts, taking into account different fuel processing strategies.

Because of the large number of variables usually considered and the mathematical models applied, classical optimization techniques may consume excessive CPU time or even prove unable to take into account all the characteristics associated with the posed problem. During the last 3 decades, heuristic techniques have been applied. One of the most used heuristic techniques has been the multi-objective evolutionary algorithms (MOEAs). Dufo and Bernal [16] applied the strength Pareto evolutionary algorithm to the multi-objective design of isolated hybrid systems, minimizing both the total cost and the unmet load. They also studied a triple multi-objective design of isolated PV–wind–diesel–hydrogen–minimized battery system and simultaneously, the total cost throughout the useful life of the installation, pollutant emissions (CO_2) and unmet load by a multi-objective evolutionary algorithm (MOEA) and a genetic algorithm (GA) [17]. Sadeghi and Ameri [18] presented a multi-objective optimization method for calculating the optimum configurations of photovoltaic–battery systems with high reliability and minimum cost for different tilt angles of the panels.

Iran holds the world's second-largest proven natural gas reserves, surpassed only by Russia in the world, and also holds the world's fourth-largest proved crude oil reserves [19]. Also, there is a natural gas pipeline in most parts of the country. On the other hand, Iran has a good solar energy potential. Therefore, using solar radiation, natural gas and petroleum products for local power generation are recommended.

In this study, the combination of photovoltaic panels (PV), coupled solid oxide fuel cell (SOFC) and gas turbine (GT), and electrolyser are considered for power generation. The number of PV panels, the maximum number of PV panels, the power of SOFC-GT, and the power of electrolyser can be changed. A multi-objective optimization method (PESA) is considered to obtain the best hybrid systems from economical, ecological, and reliability point of view. Also in this work, the effect of panel's angle changes and SOFC fuel type are considered. This study is done about two fuel prices: Iran fuel price and international fuel price.

2. SYSTEM DESCRIPTION

Figure 1. illustrates a schematic diagram of the PV-coupled SOFC and GT-electrolyser hybrid system. The proposed system consists of the PV panels, a coupled SOFC-GT system, an electrolyser, the hydrogen tanks, the inverters, and other related components.

The load demand is determined for each hour. If the generated power from PV panels is greater than the load demand, the excess power converts to hydrogen by electrolyser as much as the power of electrolyser and

stores in hydrogen tanks. If the generated power from PV panels is lower than the load demand, the remaining power is generated by SOFC-GT with hydrogen as fuel. Finally, if the stored hydrogen is not enough to generate the remaining power, SOFC-GT uses other fuels (methane, propane, diesel fuel or ethanol) to generate power. However, if the remaining power is greater than SOFC-GT power, this hour marks an unmet load. The SOFC and PV panel generated power is DC current, which is converted into the AC current by inverters.

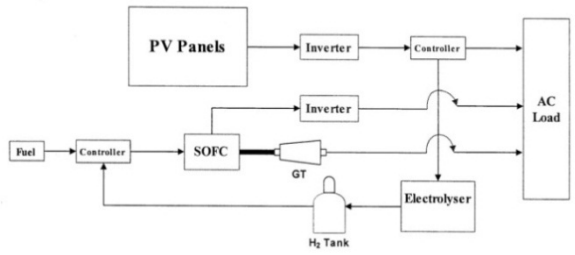

Figure 1. The hybrid power generation system.

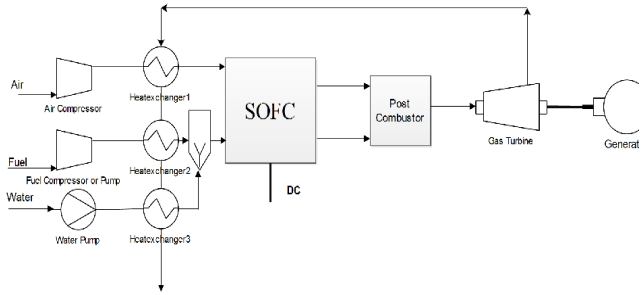

Figure 2. The coupled SOFC-Gas Turbine system with Steam Reforming.

Figure 2. illustrates a schematic diagram of the SOFC-Gas Turbine coupled system. The proposed system consists of a SOFC, a post-combustor, a gas turbine, a fuel compressor or pump, an air compressor, a water pump, some heat exchangers, and other related components.

It is obvious that fuel and air are compressed up to a SOFC stack operating pressure by the fuel compressor or fuel pump and air compressor, and are preheated in corresponding heat exchangers by the exhaust of a gas turbine. After being pressurized by the pump, the water is preheated to generate the superheated steam in the corresponding heat exchanger by the exhaust of a gas turbine. Then it is mixed with the fuel to produce a mixture that will drive the internal steam reforming reaction. The preheated air is fed to the cathode of the SOFC, and the mixture of steam and fuel is fed to the SOFC anode. The electrochemical reaction occurs to produce DC current which is converted into the AC current by an inverter. After the electrochemical reaction in the SOFC stack is finished, the excess air coming out of the cathode and the unreacted fuel coming out of the anode combust completely in a post-combustor to generate the combustion gas under high temperature and pressure, which is expanded through a gas turbine to produce power. The exhaust gas from the gas turbine is sequentially used to preheat the air, fuel, and water respectively.

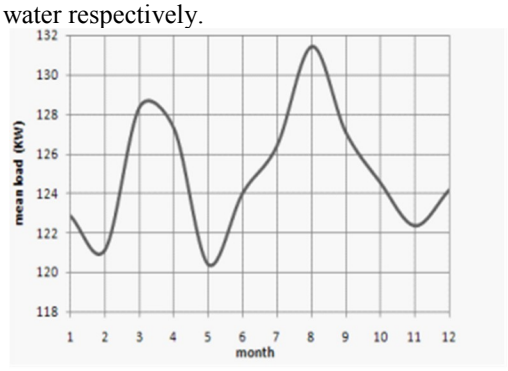

Figure 3. Monthly average hourly load.

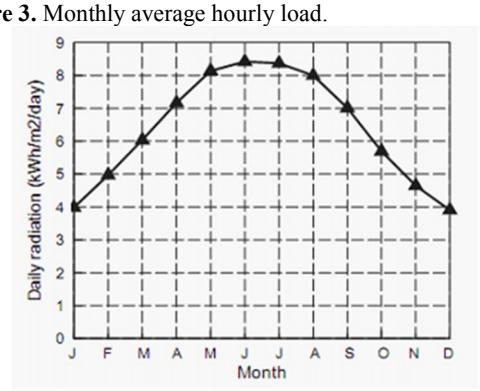

Figure 4. Monthly average daily radiation.

3. LOAD DEMAND

In the present work, load demand is a representation of remote households in Kerman, which are far from the utility grid. The measured annual average electric energy consumption of 500 typical households is considered. The diagram of sample load has been plotted in Figure 3. which shows mean electrical load for every month.

4. MATHEMATICAL MODELING OF COMPONENT

4.1. PV panels The solar energy calculations are made by using the hourly solar radiation data. The electricity generated by the PV systems is directly related to the solar energy received by the PV panels while the PV panels can be placed at different tilt angles and orientations. Most local solar observatories only provide solar irradiance data on a horizontal plane (Radiation in Kerman for different month of the year has been shown in Figure 4.) Thus, an estimate of the total solar radiation incident on any required sloping surfaces is needed. The HDKR model (Hay, Davies, Klucher, Reindl model) [20] is utilized to estimate the total solar radiation on the tilted surface:

$$I_T=(I_b+I_dA_i)R_b+I_d(1-A_i)\left(\frac{1+\cos\beta}{2}\right)\left[1+f\sin^3\left(\frac{\beta}{2}\right)\right]+(I_b+I_d)\rho_g\left(\frac{1-\cos\beta}{2}\right) \quad (1)$$

where I_b and I_d are direct normal and diffuse solar radiations. A_i is the anisotropy index, and R_b is the geometric factor, which are defined as below:

$$A_i=\frac{I_b}{I_o} \quad (2)$$

$$R_b=\frac{\cos\theta}{\cos\theta_z} \quad (3)$$

In the above relations, I_o is the integrated hourly extraterrestrial radiation on a horizontal surface; θ and θ_z are incidence and zenith angles, respectively. f is the cloudiness factor and is given by the following equation:

$$f=\sqrt{\frac{I_b}{I_b+I_d}} \quad (4)$$

In equation (1), β is the slope of PV panels and ρ_g, the ground reflectance (also called Albedo), is the fraction of solar radiation incident on the ground that is reflected. A typical value of ground reflectance for grass-covered areas is 20 per cent, snow-covered area is 70 per cent, grass-plot area is 30 per cent, and desert dry lands are 45 per cent. In this article, the ground reflectance value is considered to be 45 per cent according to the Kerman climate (dry/desert-covered area).

Hourly power output from PV system is given by:

$$P_{PV}=I_T\eta_m\eta_{pc}P_fA_{PV} \quad (5)$$

where A_{pv} is the total area of the PV modules in m^2, η_m is the module reference efficiency (0.11), P_f is the packing factor (0.91), and η_{pc} is the power conversion efficiency (0.83). The module reference efficiency η_m can be estimated from the current and voltage of the PV module at maximum power point:

$$\eta_m=Cu_{mp}V_{mp}/GA_{cs} \quad (6)$$

where Cu_{mp} is the current at maximum power point (A), V_{mp} is the voltage at maximum power point (V), and A_{cs} is the area of a single PV module (m^2). The solar radiation at reference condition G in equation (6) is $1000W/m^2$.

4.2. Auxiliary system The SOFC is a complete solid-state device uses an oxide ion-conducting ceramic material as the electrolyte. It is therefore more simple in concept than all the other fuel cell systems, as only two phases (gas and solid) are required. The high operating temperatures mean that precious metal electrocatalysts are not needed. Both hydrogen and carbon monoxide can act as fuels in the SOFC. A negatively charged ion (O=) is transferred from the cathode through the electrolyte to the anode. Thus, product water is formed at the anode. Until recently, SOFCs have all been based on an electrolyte of zirconia stabilized with the addition of a small percentage of yttria. Above a temperature of about 800◦C, zirconia becomes a conductor of oxygen ions (O=), and typically the state-of-the-art zirconia-based SOFC operates between 900 and 1000°C. This is the highest operating temperature of all fuel cells, which presents both challenges for the construction and durability, and also opportunities, for example, in combined cycle applications. A SOFC generates electrical power by continuously converting chemical energy of a fuel into electrical energy through an electrochemical reaction. The fuel cell itself has no moving parts, making it quiet and reliable. The system has higher efficiency compared to conventional combustion engines, because it is not limited by Carnot efficiencies. The power output of the SOFC is given by [21, 22]:

$$\dot{W}_{sofc}=N_{cell}V_{fc}I_{fc} \quad (7)$$

where, N_{cell} is the number of single fuel cell in the stack, V_{fc} is the cell voltage and the stack current is given by.

$$I_{fc}=i_{fc}A_{fc} \quad (8)$$

where i_{fc} is the current density and A_{fc} is the effective cross sectional area.

The gas turbine is an internal combustion engine that uses combustion products as the working fluid. The engine extracts chemical energy from fuel and converts it to mechanical energy. High temperature high-pressure gas enters a turbine, where it expands down to the exhaust pressure, producing a shaft work output in the process. The turbine shaft work is used to drive the compressor and the electric generator that is coupled to the shaft. It is assumed that the cycle reaches a steady state; the pressure drops in the connection tubes are neglected; there is no heat transfer with the environment; and the gas turbine and compressors have a given isentropic efficiency, respectively. The SOFC outlet gas enters post-combustor. It is assumed that the combustion process is performed adiabatically and completely. The isentropic efficiency of the turbine is [23]:

$$\eta_{GT}=\frac{\bar{h}_{in}-\bar{h}_{out}}{\bar{h}_{in}-\bar{h}_{out,s}} \quad (9)$$

The generating power can be given as:

$$\dot{W}_{GT}=\dot{n}(\bar{h}_{in}-\bar{h}_{out}) \quad (10)$$

The isentropic efficiency of compressors or pump is:

$$\eta_{com\ or\ pump}=\frac{\bar{h}_{out,s}-\bar{h}_{in}}{\bar{h}_{out}-\bar{h}_{in}} \quad (11)$$

The actual compression power is:

$$\dot{W}_{com}=\dot{n}(\bar{h}_{out}-\bar{h}_{in}) \quad (12)$$

$$\dot{W}_{pump}=\dot{n}v(P_{out}-P_{in}) \quad (13)$$

Table 1. shows the Operating parameters of coupled SOFC-Gas Turbine system.

The specific fuel consumption is defined as the fuel consumption required to produce 1 kWh of energy, and it is equal to the hourly fuel consumption for supplying a given load during 1 h. According to Skarstein and Uhlen [24], the hourly fuel consumption can be approximated as follows:

$$F.C.=A\times P(t)+B\times P_n \quad (14)$$

Where A and B≈0 are constants that are different for various fuels, P(t) is the power generated at t moment, and P_n is the rated/nominal power.
The rate of SOFC hydrogen usage in moles per second is:

$$H_2 usage=\frac{\dot{W}_{sofc}}{2V_{fc}FU_f} \quad (15)$$

where F is the Faraday constant and U_f =0.85 is the fuel utilization.
The rate of SOFC fuel consumption in moles per second is given as:

$$Fuel\ Consumption=\frac{\dot{W}_{sofc}}{2nV_{fc}FU_f} \quad (16)$$

where n is the sum of the number of H_2 and CO that yield from reforming of one mole of fuel.
The rate of SOFC-GT fuel consumption in moles per second is given as:

$$Fuel\ Consumption=\frac{\dot{W}_{total}}{2nrV_{fc}FU_f} \quad (17)$$

where r is the ratio of SOFC-GT power to SOFC power that depends on the type of fuel and the type of SOFC reforming. Table (2) shows the constant of A that is obtained from equation (30) and the constant of r.

TABLE 1. Operating parameters of coupled SOFC-Gas Turbine system.

Ambient temperature (K)	298
Ambient pressure (bar)	1.013
Fuel compressor isentropic efficiency	0.85
Air compressor isentropic efficiency	0.85
Turbine isentropic efficiency	0.87
Pump isentropic efficiency	0.87
Inverter efficiency	0.92
SOFC operating pressure (bar)	3.432
SOFC operating temperature (K)	1173
SOFC fuel utilization factor	0.85
Cell operating voltage (v)	0.6
SOFC effective cross sectional area (m^2)	0.05
SOFC operating current density (A/m^2)	3330

4.3. Electrolyser Electrolysis is an electrochemical process in which electrical energy is the driving force of chemical reactions. The electrolysis of water is considered a well-known principle to produce oxygen and hydrogen gas. The core of an electrolysis unit is an electrochemical cell, which is filled with pure water and has two electrodes connected with an external power supply.
At a certain voltage, which is called critical voltage, between both electrodes, the electrodes start to produce hydrogen gas at the negatively biased electrode and oxygen gas at the positively biased electrode. The amount of gases produced per unit time is directly related to the current that passes through the electrochemical cell. Typical cell voltages are 1.80 to 2.05 V [25]. Electricity requirement is about 4.6 kWh/Nm^3H_2.

4.4. Inverter A power inverter, or inverter, is an electrical device that changes direct current (DC) to alternating current (AC); the converted AC can be at any required voltage and frequency with the use of appropriate transformers, switching, and control circuits. In this study ten 10KW inverter with 92% efficiency have been used.

5. OBJECTIVE FUNCTIONS

The objective functions are:
The CO_2 emission: (kg/year).
The annualized cost: ANC ($/year).
The loss of power supply percent: LPSP (%).

5.1. CO_2 Emissin Table 3. shows CO2 emission for different fuels. The hours of auxiliary systems operation and therefore, fuel consumptions are specified, so emission of different auxiliary systems will be determined.

5.2. Annualized cost In finance, the annualized cost is the cost per year of owning and operating an asset over its entire lifespan. ANC is often used as a decision making tool when comparing investment projects of unequal lifespans. In the present study, to compare different configurations of economical aspects, annualized cost is used. In order to calculate ANC, annualized initial capital cost, annualized replacement cost, and annualized operating and maintenance cost will be added.
Annualized initial capital cost:

$$C_{acap}=C_{cap}.CRF(i,R_{proj}) \quad (18)$$

C_{acap}, C_{cap}, CRF, i, R_{proj} are annualized initial capital cost, initial capital cost, capital recovery factor, real interest rate, and system lifespan respectively.

$$\text{Real interest rate: } i=\frac{f-i'}{f+1} \quad (19)$$

i' and f are nominal interest rate and inflation, respectively.
Capital recovery factor:

$$CFR(i,R_{proj})=\frac{i(1+i)^{R_{proj}}}{(1+i)^{R_{proj}}-1} \quad (20)$$

Annualized replacement cost:

$$C_{arep}=C_{rep}.f_{rep}.SFF(i,R_{comp})\text{-}S.SFF(i,R_{proj}) \quad (21)$$

C_{arep}, C_{rep}, f_{rep}, SFF, R_{comp}, S are annualized replacement cost, replacement cost, ratio of capital recovery factor,

sinking fund factor, and lifespan of component and salvage value, respectively.
Sinking fund factor:

$$SFF(i,N)=\frac{i}{(1+i)^N-1} \quad N=R_{comp},R_{proj} \tag{22}$$

Salvage value:

$$S=C_{rep}\times\frac{R_{rem}}{R_{comp}} \quad R_{rem}=R_{comp}-(R_{proj}-R_{rep})$$

$$R_{rep}=R_{comp}\times INT(\frac{R_{proj}}{R_{comp}}) \tag{23}$$

Ratio of capital recovery factor:

$$f_{rep}=\begin{cases}CRF(i,R_{proj})/CRF(i,R_{rep}) & \text{if } R_{rep}>0\\ 0 & \text{if } R_{rep}=0\end{cases} \tag{24}$$

Operating and maintenance costs are usually annualized.
Annualized cost:

$$ANC=C_{acap}+C_{arep}+C_{a\ O\&M} \tag{25}$$

Fuel prices in Iran and other places are different. In the present study, the comparison is done based on two fuel prices:
1. Iran fuel price
2. International fuel price
Table 4. shows the fuel prices. Table (5) shows the initial, replacement, operation and maintenance cost of different components. This table also shows life span and power of the components.

TABLE 2. constants for different fuels

	Hydrogen	**Methane**	**Propane**	**Ethanol**	**Diesel fuel**
Constant of A	0.558 (m^3.KW/h)	0.155 (m^3.KW/h)	0.213 (lit.KW/h)	0.227 (lit.KW/h)	0.148 (lit.KW/h)
Constant of r	1.6112	1.4528	1.4789	1.5716	1.5078
$\dot{W}_{net,T}$(KW)/500 KW Hybrid system	189.67	155.86	161.91	181.85	168.39

TABLE 3. CO2 emission per unit fuel consumption for different fuels

	CO_2 emission
Methane	1.782 (kg/m^3 Methane)
Propane	1.53 (kg/lit Propane)
Ethanol	1.497 (kg/lit Ethanol)
Diesel Fuel	2.329 (kg/lit Diesel fuel)

TABLE 4. Different fuel prices

	International fuel price [26]	Iran fuel price [27, 28]
Methane	0.123($/$m^3$)	0.084($/$m^3$)
Propane	0.232($/lit)	0.04($/lit)
Ethanol	0.667($/lit)	0.74($/lit)
Diesel Fuel	0.852($/lit)	0.14($/lit)

TABLE 5. Specifications of different components [29, 30]

	Power	Initial capital cost ($/KW)	Replacement cost ($/KW)	O&M cost per year ($/KW)	Life span (years)
PV panel	200 W	1000-3000	0	0.0025	25
Electrolyser	-	450	405	0.1	15
Inverter	10×10 KW	200-400	180-360	0.0015	15
SOFC-GT	-	1100	990	0.0086	15

5.3. Loss of power supply percent Reliability of the system is expressed in terms of loss of power supply percent (LPSP). The objective function, LPSP, can be described by:

$$LPSP=\frac{\sum_{t=1}^{N_h}\text{hours}[P_{supply}(t)<P_{needed}(t)]}{N_h}\times 100 \tag{26}$$

In the above relation, N_h is the number of time intervals (8760, number of hours in a year).

6. MULTI-OBJECTIVE OPTIMIZTION EVOLUTIONARY ALGORTHIM

In this section, the multi-objective design problem is mathematically formulated and the basic concepts used by the MOEAs are defined. Finally, the applied MOEA (PESA) is also described, which searches the best combination of components minimizing ANC, and pollutant emissions. A multi-objective optimization problem can be defined as follows:
Minimize or maximize the objective functions included in the vector:
$F(x)=\{f_1(x),f_2(x),\ldots,f_k(x)\}$
Satisfying the m restrictions of inequality and the p restrictions of equality:

$g_i(x) \geq 0 \quad i=1,2, \ldots,m$
$h_i(x)=0 \quad i=1,2, \ldots, p$
Where x is a vector whose elements are the decisive variables of the problem.
Concepts related to Pareto optimality are regularly used in most MOEAs. Because of this, the concepts of Pareto dominance, Pareto optimality, Pareto optimal set, and Pareto front are defined.
Pareto dominance: a vector $u = (u_1, u_2,\ldots, u_k)$ is said to dominate $v = (v_1, v_2,\ldots, v_k)$ (denoted by $u \preccurlyeq v$) if and only if u is partially less than v, i.e.,
$\forall i \in \{1,2,\ldots,k\}: u_i \preccurlyeq v_i \wedge \exists i \in \{1,2,\ldots,k\}: u_i \prec v_i$
Pareto optimality: a solution $x \in \Omega$ is said to be Pareto optimal with respect to Ω if and only if there is no $x' \in \Omega$ for which $v=F(x')=(f_1(x'),f_2(x'),\ldots,f_k(x'))$ dominates $u=F(x)=(f_1(x),f_2(x),\ldots,f_k(x))$.
Pareto optimal set: for a given MOP F(x), the Pareto optimal set (P*) is defined as follows:
$P^*=\{x \in \Omega \mid \exists x' \in \Omega : F(x') \preccurlyeq F(x)\}$
Pareto front: for a given MOP F(x) and Pareto optimal set P*, the Pareto front (PF*) is defined as follows:
$PF^*=\{u= F(x)=(f_1(x), f_2(x), \ldots, f_k(x)) x \in P^*\}$
The implemented multi-objective algorithm is based on PESA that is presented by Corne et al [31]. It has approximately fast convergence, probably due to its higher elitism intensity and it also has good accuracy. PESA has two parameters concerning population size i.e PI (the size of the internal population IP) and PE (the maximum size of the archive or external population). It has one parameter concerning the hyper-grid crowding strategy. The main steps in this algorithm are (i) Generate and evaluate each of an initial internal population (IP) of PI chromosomes and initialize the external population (EP) to the empty set.(ii) Incorporate the non-dominated members of IP into EP.(iii) If a termination criterion has reached then stop, returning the set of chromosomes in EP as the result. Otherwise, delete the current contents of IP and repeat the following until PI new candidate solutions have been generated. With probability P_c, select two parameters from EP. Produce a single child via uniform crossover and mutate the child via bit-flip mutation. With probability $(1-P_c)$ select one parent and mutate it to produce a child. (iv) Repetition of the same process.
1. Generate and evaluate each of an initial internal population (IP) of PI chromosomes.
2. Initialize the external population (EP) as empty set.
3. For t=1 to Number of Generations
3.1. Incorporate the non-dominated members of IP into EP.
3.2. Delete the current content of IP.
3.3. Until obtaining new solution of PI.
3.3.1. Select two parents from EP with probability P_c
3.3.2. Recombine these two parents for obtaining one offspring
3.3.3. Mutate the offspring
3.3.4. Select one parent from IP with probability $(1-P_c)$
3.3.5. Mutate the parent to produce one offspring
3.3.6. Add the two obtained offspring into IP
4. Return to 3
This algorithm is in charge of finding the designs that manage to, simultaneously, minimize the ANC of the system, and the pollutant emissions. It has been developed using the MATLAB programming language. The algorithm (MOEA) can search for the configuration of PV panels, auxiliary system, and inverter which minimizes three objectives mentioned.

7. RESULTS

The energy from sunlight reaching the earth is a free and huge source of energy that can be exploited and used for generating electricity by photovoltaic panels. Given the discontinuous nature of solar energy, the use of a storage device to store energy during the day and supply it at night is essential. The storage device in this study is an electrolyser and H_2 tanks. Moreover, using an auxiliary system is necessary to increase the reliability of the power generation system and cloudy days. One of the most efficient auxiliary systems is coupled SOFC-GT. This work, in addition to introducing this new hybrid system, explains the effect of different conditions on it. The most desirable hybrid system is the low cost and the least emission one. But cost and emission are in conflict with each other. In order to obtain optimum solutions (Solutions are different in the number of PV panels and the power of electrolyser), a multi-objective optimization (PESA) is used. Because of the SOFC operating conditions, various fuels can be used. Four specific fuels are considered to determine the best fuel from ecological and economical point of view. Diesel fuel: that is a portable and storable in liquid fuel tanks, and a conventional liquid fuel. Ethanol: that is a renewable fuel made from corn and other plant materials. Propane: a fossil fuel which is portable and storable in pressure vessels. Methane: a gas fuel which is transportable by pipelines.
Each photovoltaic panel occupies about 1.5 m^2, so the maximum number of panels (MNP) is limited. The effect of this limitation has been considered in this study. Figure 5. shows the Pareto frontiers of four fuels for two different situations, when the maximum number of panels is limited to 1000 and when it is limited to 3000. This figure is for international fuel price, and the power of auxiliary system is considered 500KW. The international price of diesel fuel and ethanol is more than methane and propane. Figure 5. shows that when the MNP decreases, the number of optimum solutions becomes limited, i.e. the solutions with more cost and lower emission are removed. It is obvious that when the fuel price is high and the MNP is 1000, the Pareto frontier becomes a point. The operation of the auxiliary

system and so the emissionincrease when the number of panels is less than 1000. On the other hand, because of the high fuel price, the annualized cost increases. As a result, annualized cost and emission are both increase and therefore, optimization algorithm selects the hybrid system with 1000 PV panels only; however, when the number of panels is more than 1000, the effect of the panel cost is greater than the effect of fuel price so, the Pareto frontier contains more than one solution. The difference between Figure 6. and Figure 5. is that Figure 6. is obtained for Iran fuel prices. Diesel fuel price is lower in Iran so the Pareto frontier of diesel fuel is similar to that of methane and propane. Therefore, the number of optimal solutions depends on the fuel price and MNP. Table 6. shows some of the results with approximately the same number of PV panels for comparison. The MNP is considered 3000 for the rest of the results of this study. Electing an appropriate power for the auxiliary system is very important. If the power of the auxiliary system is low, LPSP of the system increases i.e. the reliability of the system decreases. And if the power of the auxiliary system is high, annualized cost and emission of the system increase without any effect on its reliability. Figure 7. shows the Pareto frontiers of methane for four different power of auxiliary system in international fuel price. It is obvious that when the power of the auxiliary system decreases, annualized cost and emission will decrease. But as it is seen in Table 7. LPSP will increase when the power of the auxiliary system decreases. Table 7. shows that the optimum power for the auxiliary system is 500KW. Figure 8. shows the Pareto frontiers of methane for four different power of the auxiliary system in Iran fuel price, and Figure 9. shows the Pareto frontiers of diesel fuel for four different power of the auxiliary system in international fuel price. From Figures 8. and 9. it can be concluded that the fuel type and the fuel price do not influence the election of the power of the auxiliary system. The power of the auxiliary system is considered 500KW for the rest results of this study. Figure 10. shows the Pareto frontiers for four different fuels in international fuel price. It is obvious that methane is the best and ethanol is the worst fuel from ecological and economical points of view. But ethanol is a renewable fuel made from corn and other plant materials. Plants convert CO_2 to O_2 in photosynthesis process. Therefore, the ethanol production process decreases CO2 emission but calculation of this reduction is difficult and it is not considered in this study. Because of this and according to the depletion of fossil fuel reserves, the renewable sources of energy will be in more attention in the near future.

According to Figure 10. for places without gas pipeline, the best fuel is propane. Figure 11. compares these four fuels in Iran fuel price. Due to the lower price of diesel fuel in Iran, the difference between the Pareto frontiers of diesel fuel and propane in Figure 11. is less than that in Figure 10.

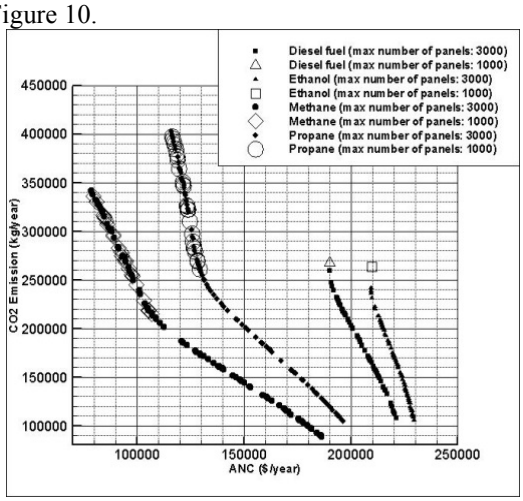

Figure 5. Pareto frontier of hybrid system for four fuels with different MNP, International fuel price, 500KW SOFC-GT.

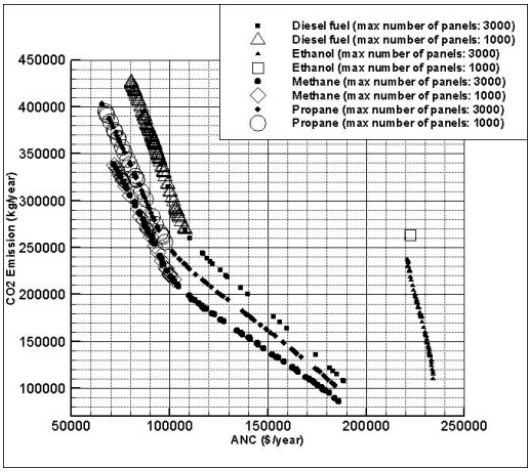

Figure 6. Pareto frontier of hybrid system for four fuels with different MNP, Iran fuel price, 500KW SOFC-GT.

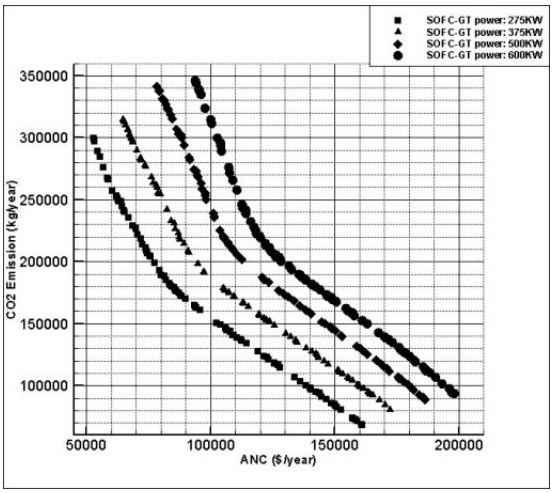

Figure 7. Pareto frontier of hybrid system for methane with different power of APS, International fuel price, MNP:3000.

TABLE 6. Some of the optimum results for 500KW hybrid system

	MNP	Fuel	ANC ($/year)	CO2 emission (kg/year)	Number of panel	Power of electrolyser (KW)
International fuel prices	1000	CH_4	106908	214848	994	110
		C_3H_8	130049	255383	977	110
		C_2H_5OH	209658	263259	1000	110
		$C_{12}H_{26}$	190058	267187	999	110
	3000	CH_4	186247	88333	2958	490
		C_3H_8	196033	104653	2950	490
		C_2H_5OH	229284	105394	2998	500
		$C_{12}H_{26}$	217835	96213	2963	520
Iran fuel prices	1000	CH_4	102311	214103	999	110
		C_3H_8	98671	253449	993	110
		C_2H_5OH	222578	263610	1000	110
		$C_{12}H_{26}$	107919	269319	986	110
	3000	CH_4	185978	86150	2990	500
		C_3H_8	183936	102957	2974	500
		C_2H_5OH	234100	109749	2943	490
		$C_{12}H_{26}$	188460	107294	2991	500

TABLE 7. Some of the optimum results for different power of auxiliary power system (APS)

	Power of APS(KW)	**Fuel**	ANC ($/year)	CO2 emission (kg/year)	Number of panel	Power of electrolyser (KW)	LPSP
International fuel prices	275	CH_4	123326	121249	2023	310	5%
		$C_{12}H_{26}$	170244	152272	2011	310	5%
	375	CH_4	134474	135680	2015	310	1%
		$C_{12}H_{26}$	187005	169482	2013	310	1%
	500	CH_4	148068	147169	2009	310	0%
		$C_{12}H_{26}$	205056	183006	2016	310	0%
	600	CH_4	160875	152740	2051	320	0%
		$C_{12}H_{26}$	219277	192780	2022	310	0%
Iran fuel prices	275	CH_4	120776	121075	2027	310	5%
		$C_{12}H_{26}$	124175	151311	2023	310	5%
	375	CH_4	131282	136278	2006	310	1%
		$C_{12}H_{26}$	136335	167525	2041	310	1%
	500	CH_4	144649	147700	2001	310	0%
		$C_{12}H_{26}$	152077	177707	2089	320	0%
	600	CH_4	157740	152402	2059	320	0%
		$C_{12}H_{26}$	161175	191669	2042	320	0%

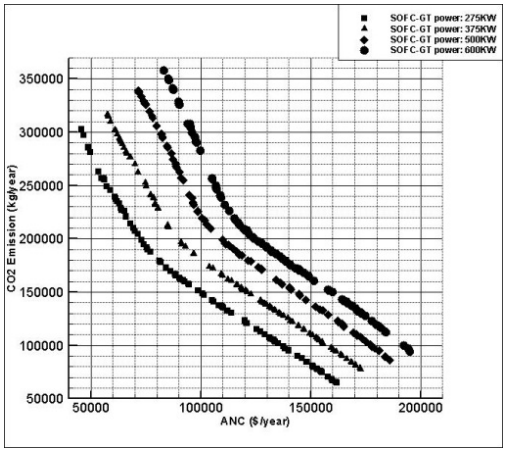

Figure 8. Pareto frontier of hybrid system for methane with different power of APS, Iran fuel price, MNP:3000.

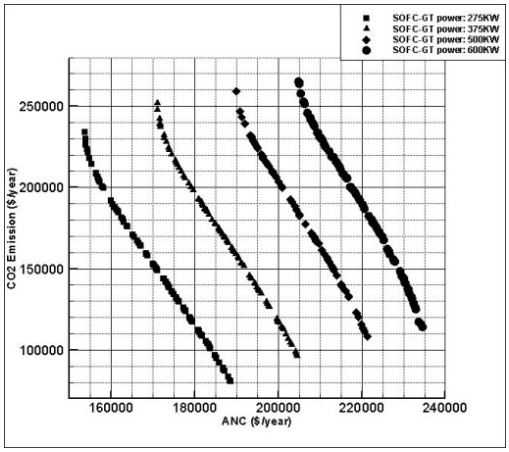

Figure 9. Pareto frontier of hybrid system for diesel fuel with different power of APS, International fuel price, MNP:3000.

If the panel angle changes and tracks the sun, PV panel productivity increases and the number of panels decreases, so the annualized cost are reduced. In this study, the effect of seasonal and monthly panel angle change is considered. The best panel angle in Kerman (30°15'N, 56°58'E), Iran, for the most productivity in different months and seasons are brought in Tables (8,9).

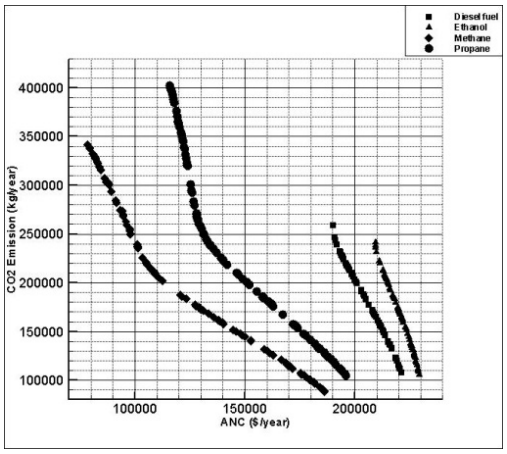

Figure 10. Pareto frontier of hybrid system for four fuels, International fuel price, 500KW SOFC-GT, MNP:3000.

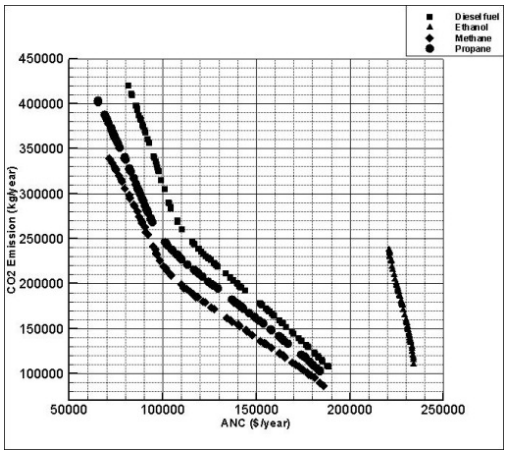

Figure 11. Pareto frontier of hybrid system for four fuels, Iran fuel price, 500KW SOFC-GT, MNP:3000.

These angles determined by comparing the received solar radiation for different tilt angles in every month or every season [18]. The optimum panel angle in Kerman for fixed panel angle situation is about the latitude of Kerman (30°) [32]. Figure 12. shows the effect of panel angle change on the hybrid system in international fuel price for methane. It shows that the effect of panel angle change is negligible specially when the number of panels decreases. Figure13. shows the effect of panel angle change in Iran fuel price situation for methane. Its results are the same as Figure 12. Figure 14. is plotted for diesel fuel. It is obvious that when the fuel price is high, the hybrid system goes to select more panels and so the effect of panel angle change increases, as much as, the difference between seasonal and monthly changes of panel angle are observable.

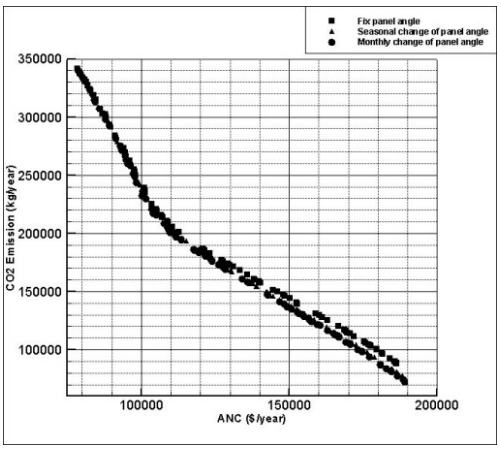

Figure 12. Pareto frontier of hybrid system for methane with fix, seasonal, and monthly panel angle change, International fuel price, 500KW SOFC-GT, MNP:3000.

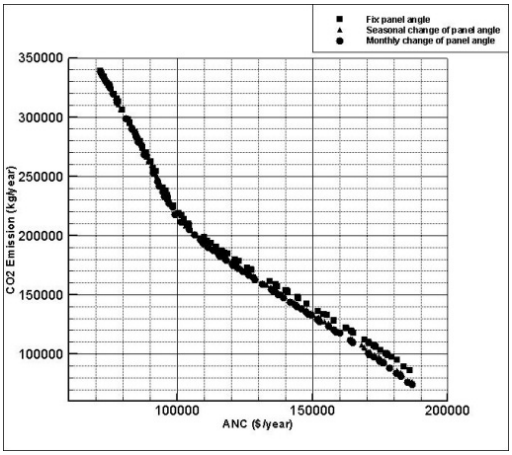

Figure 13. Pareto frontier of hybrid system for methane with fix, seasonal, and monthly panel angle change, Iran fuel price, 500KW SOFC-GT, MNP:3000.

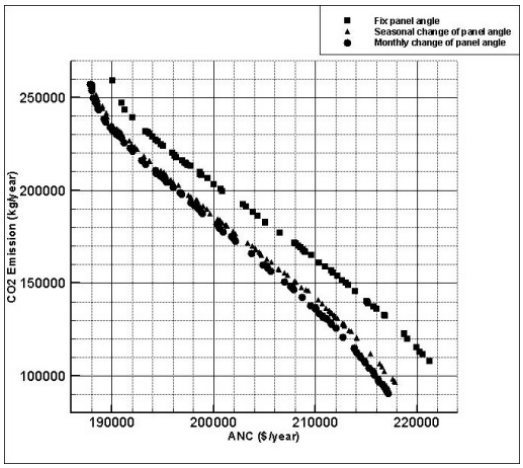

Figure 14. Pareto frontier of hybrid system for diesel with fix, seasonal, monthly panel angle change, International fuel price, 500KW SOFC-GT, MNP:3000.

TABLE 8. Best tilt angle for different month of year

Month	1	2	3	4	5	6	7	8	9	10	11	12
Panel tilt angle (°)	55	50	35	20	10	10	10	15	30	45	55	60

TABLE 9. Best tilt angle for different season of year

Season	Winter	Spring	Summer	Autumn
Panel tilt angle (°)	45	10	15	55

8. CONCLUSION

This hybrid system is a practical system for generating a load demand. The number of optimal solutions depends on the fuel price and MNP. If the power of the auxiliary system is high, the annualized cost and the emission of the system increase, and if it is low, the reliability of the system decreases, so the power of the auxiliary system should always be elected optimally. Methane is the best fuel for this hybrid system economically and ecologically. But if there is no gas pipeline, the best alternative fuel is propane. Seasonal or monthly change of panel angle affects the system when the fuel price is high or when the number of panels increases.

REFERENCES

1. Baniasad Askari, I. and Ameri, M., "Optimal sizing of photovoltaic–battery power systems in a remote region Kerman, Iran", ***Part A Journal of Power Energy,*** Vol. 223, No. 5, (2009), 563-570.
2. Nafeh, A.A, "Proposed Technique for Optimally Sizing a PV/Diesel Hybrid System", ***International Conference on Renewable Energies and Power Quality,*** Spain, (2010).
3. Dufo-Lopez, R. and Bernal-Agust, J.L., "Design and Control Strategies of PV-Diesel Systems Using Genetic Algorithms", ***Solar Energy,*** Vol. 79, No. 1, (2005), 33-46.
4. Tudorache, T. and Morega, A., "Optimum Design of Wind/PV/Diesel/Batteries Hybrid Systems", ***2ND International Conference on Modern Power Systems in Romania,*** (2008), 261-264.
5. Rehman, S. and Al-Hadhrami, L.M., "Study of a solar PV-diesel-battery hybrid power system for a remotely located population near Rafha, Saudi Arabia", ***Energy,*** Vol. 35, No. 12, (2010), 4986-4995.
6. Khatiba, T., Mohameda, A., Sopianb, K. and Mahmoud, M., "Optimal sizing of building integrated hybrid PV/diesel generator system for zero load rejection for Malaysia" ***Energy and Buildings,*** Vol. 43, No. 12, (2011), 3430-3435.
7. Yamegueu, D., Azoumah, Y., Py, X. and Zongo, N., "Experimental study of electricity generation by Solar PV/diesel hybrid systems without battery storage for off-grid areas", ***Renewable Energy,*** Vol. 36, (2011), 1780-1787.
8. Baniasad Askari, I. and Ameri, M., "The Effect of Fuel Price on the Economic Analysis of Hybrid (Photovoltaic/Diesel/Battery) System in Iran", ***Journal of Energy Sources,*** part B: Economics, Planning, and Policy, Vol. 6, (2011), 357-377.
9. Nabil, A.A., Miyatake, M. and Al-Othman, A.K., "Power fluctuations suppression of stand-alone hybrid generation combining solar photovoltaic/wind turbine and fuel cell systems", ***Energy Conversion and Management,*** Vol.49, (2008), 2711–2719.
10. Sergio, B., Silva, S.B., de-Oliveira, M.A. G. and Severino, M.M., "Economic evaluation and optimization of a photovoltaic–fuel cell–batteries hybrid system for use in the Brazilian Amazon", ***Energy Policy,*** Vol. 38, (2010), 6713-6723.
11. Eroglu, M., Dursun, E., Sevencan, S., Song, J., Yazici, S. and Kilic, O., "A mobile renewable house using PV/wind/fuel cell hybrid power system" ***International Journal of Hydrogen Energy,*** Vol. 36, (2011), 7985-7992.
12. Lee, B., Park, P., Kim, C., Yang, S. and Ahn, S., "Power managements of a hybrid electric propulsion system for UAVs", ***Mechanical Science and Technology,*** Vol. 26, No. 8, (2012), 2291-2299.
13. Sadeghi, S. and Ameri, M., "Comparison of Different Power Generators in PV-Battery-Power Generator Hybrid System", ***Mechanical Science and Technology,*** Vol. 28, No. 1, (2014), 387-398
14. Cheddie, F. D., "Thermo-economic optimization of an indirectly coupled solid oxide fuel cell/gas turbine hybrid power plant", ***International Journal of Hydrogen Energy,*** Vol. 36, (2011), 1702-1709.
15. Santin, M., Traverso, A., Magistri, L. and Massardo, A., "Thermoeconomic analysis of SOFC-GT hybrid systems fed by liquid fuels", ***Energy,*** Vol. 35, (2010), 1077–1083.
16. Bernal-Agust, J.L. and Dufo-Lopez, R., "Multi-objective design and control of hybrid systems minimizing costs and unmet load", ***Electric Power Systems Research,*** Vol. 79, (2009), 170–180.
17. Dufo-Lopez, R. and Bernal-Agust, J.L., "Multi-objective design of PV–wind– diesel– hydrogen– battery systems", ***Renewable Energy,*** Vol. 33, (2008), 2559– 2572.
18. Sadeghi, S. and Ameri, M., "Multi-objective Optimization of PV-Battery Power Systems", ***20th Annual International Conference on Mechanical Engineering of Iran,*** (2012).
19. http://www.eia.gov/beta/international/analysis.cfm?iso=IRN
20. Duffie, J.A. and Beckman, W.A., "Solar engineering of thermal process", (1990) 2nd Ed., Wiley, NewYork.
21. Yu, Z., Han, J. and Cao, X., "Investigation on performance of an integrated solid oxide fuel cell and absorption chiller tri-generation system", ***International Journal of Hydrogen Energy,*** Vol. 36, No. 19, (2011), 12561-12573.
22. Ma, S., Wang, J., Yan, Z., Dai, Y. and Lu, B., "Thermodynamic analysis of a new combined cooling, heat and power system driven by solid oxide fuel cell based on ammonia–water mixture", ***Journal of Power Sources,*** Vol. 196, No. 20, (2011), 8463– 8471.
23. Stamatis, A., Vinni, C., Bakalis, D., Tzorbatzoglou, F. and Tsiakaras, P., "Exergy Analysis of an Intermediate Temperature Solid Oxide Fuel Cell-Gas Turbine Hybrid System Fed with Ethanol", ***Energies,*** Vol. 5, (2012), 4268-4287.
24. Skarstein, O. and Uhlen, K., "Design considerations with respect to long-term diesel saving in wind/diesel plants", ***Wind Engineering,*** Vol. 13, (1989), 72-87.
25. http://www.ieahia.org.

26. http://www.indexmundi.com/commodities/?commodity=natural-gas.

27.http://web.archive.org/web/20140419142841/http://sedaghatnews.ir/Pages/News-7244.html.

28. http://web.archive.org/web/20130504035631/http://www.epa-iran.ir/farsi/news/prices1391.html.

29. http://www.wholesalesolar.com

30. Mekhilef, S., Saidurb, R. and Safari, A., "Comparative study of different fuel cell technologies", ***Renewable and Sustainable Energy Reviews,*** Vol. 16, No. 1, (2012), 981–989.

31. Corne, W., Knowles, D. and Oates, J., "The Pareto envelope-based selection algorithm for multi objective optimization", ***Lecture Notes in Computer Science,*** Vol. 1917, (2000), 839-848.

32. Jamil Ahmad, M. and Tiwari, G.N., "Optimization of Tilt Angle for Solar Collector to Receive Maximum Radiation", ***The Open Renewable Energy Journal,*** Vol. 2, (2009), 19-24.